

Graph Neural Networks for Surfactant Multi-Property Prediction

Christoforos Brozos^{a,b}, Jan G. Rittig^b, Sandip Bhattacharya^a, Elie Akanny^a, Christina Kohlmann^a,
Alexander Mitsos^{d,b,c,*}

^a BASF Personal Care and Nutrition GmbH, Henkelstrasse 67, 40589 Duesseldorf, Germany

^b RWTH Aachen University, Process Systems Engineering (AVT.SVT), Aachen, Germany

^c Forschungszentrum Jülich GmbH, Institute for Energy and Climate Research IEK-10: Energy Systems Engineering, Jülich, Germany

^d JARA Center for Simulation and Data Science (CSD), Aachen, Germany, Aachen, Germany

Abstract

Surfactants are of high importance in different industrial sectors such as cosmetics, detergents, oil recovery and drug delivery systems. Therefore, many quantitative structure-property relationship (QSPR) models have been developed for surfactants. Each predictive model typically focuses on one surfactant class, mostly nonionics. Graph Neural Networks (GNNs) have exhibited a great predictive performance for property prediction of ionic liquids, polymers and drugs in general. Specifically for surfactants, GNNs can successfully predict critical micelle concentration (CMC), a key surfactant property associated with micellization. A key factor in the predictive ability of QSPR and GNN models is the data available for training. Based on extensive literature search, we create the largest available CMC database with 429 molecules and the first large data collection for surface excess concentration (Γ_m), another surfactant property associated with foaming, with 164 molecules. Then, we develop GNN models to predict the CMC and Γ_m and we explore different learning approaches, i.e., single- and multi-task learning, as well as different training strategies, namely ensemble and transfer learning. We find that a multi-task GNN with ensemble learning trained on all Γ_m and CMC data performs best. Finally, we test the ability of our CMC model to generalize on industrial grade pure component surfactants. The GNN yields highly accurate predictions for CMC, showing great potential for future industrial applications.

1 Introduction

Surfactants are highly relevant molecules used in a wide range of everyday products, such as food, cosmetics, detergents and drugs (Vieira et al., 2021; Shaban et al., 2020; Nitschke and Costa, 2007; Tadros, 2005; Adu et al., 2020; Szűts and Szabó-Révész, 2012). Surface-active agents (surfactants) are amphiphilic molecules with a hydrophobic chain and a polar hydrophilic head. The surfactant molecule orients itself at the interface between two phases with the hydrophobic portion oriented towards the hydrophobic phase (e.g., air/oil) and the hydrophilic portion oriented towards the hydrophilic phase. Due to their structure, surfactants are surface/interface active and they are able to lower the surface/interfacial tension (Shaban et al., 2020; Zhang et al., 2019). Owing to their properties, surfactants are widely used in a variety of applications such as detergents, dispersion stabilizers, foaming agents, lubricants and as pharmaceuticals among many others (Knop et al., 2010; Shaban et al., 2020; Schramm et al., 2003; Gallou et al., 2015). Surfactants are classified based on their hydrophilic head group, into ionics and nonionics, with the former further classified into anionics, cationics and zwitterionics. Important surfactant properties to various applications are the critical micelle concentration (CMC), the surface tension (γ), the surface excess concentration (Γ_m), the Cloud Point (CP) and the Krafft Temperature (KT) (Yang and Brouillette, 2016; Al-Sabagh et al., 2011). These properties are used to identify new surfactants with desired performance.

Amphiphilic molecules such as surfactants form micelles, i.e., aggregates. Micelles ultimately dictate the surface/interface activity and strongly impacts the solubilization and detergency, or cleaning ability of a surfactant solution (Patist et al., 2001). The minimum surfactant concentration at which such micelles are formed in a solution is called *critical micelle concentration* (CMC) (Rosen and Kunjappu, 2012; Mukerjee and Mysels, 1971). The CMC is an important value in a wide range of applications such as shampoos (Thompson et al., 2023), bio-materials design for drug delivery systems (Su et al., 2020), polymeric micelles (Ghezzi et al., 2021; Perumal et al., 2022) and oil recovery (Kumar and Mandal, 2019). In addition, some studies have reported correlation between CMC and surfactant toxicity (Perinelli et al., 2016) and between CMC and foam stability (Majeed et al., 2020). The CMC is influenced by multiple

* Corresponding author, E-mail: amitsos@alum.mit.edu

factors, like temperature, solvent, pH, chemical structure, pressure conditions and size of the tail and head groups (Katritzky et al., 2008; Thiruvengadam et al., 2020; Rosen and Kunjappu, 2012). Determination of CMC is time-consuming and expensive, and several methods can be used like tensiometry (Dahanayake et al., 1986), refractive index (Mukerjee and Mysels, 1971), calorimetry (Ortona et al., 1998), viscosity and conductivity measurements (Jobe and Reinsborough, 1984). In most methods, a break-point in the measured property (e.g., surface tension or conductivity) vs. surfactant concentration curve is observed, and the CMC is defined to be at that point (Mukerjee and Mysels, 1971; Perinelli et al., 2020; Moulik et al., 2021).

Since surfactants prefer to exist and adsorb at the interfaces, we can define their adsorption effectiveness as the surface excess concentration (Γ_m) (Rosen and Kunjappu, 2012). Γ_m is an important surfactant property, as it is a measure of surfactant concentration at air/water and oil/water interfaces. Additionally, surface excess concentration has been shown to influence foaming, emulsification and the kinetics of surfactant-induced pore wetting (Rosen and Kunjappu, 2012; Wang et al., 2019). Like CMC, Γ_m is influenced by surfactant structure and temperature (Myers, 2020; Rosen and Kunjappu, 2012). The implicit calculation of the surface excess concentration is possible, as is the CMC, from a surface tension measurement plot using the Gibbs adsorption equation (Rosen et al., 1982a; Rosen and Kunjappu, 2012).

Due to the tedious and expensive nature of experiments, the prediction of surfactant properties without experiments has been a focus of research for many years, mainly, through the use of quantitative structure-property relationship (QSPR) models. An overview of QSPR models in surfactants was given by Hu et al. (2010), with most of the QSPR studies aiming to correlate molecular descriptors with the CMC (Gaudin et al., 2016; Katritzky et al., 2008; Mattei et al., 2013). The developed models showed good predictive performance (Gaudin et al., 2016; Katritzky et al., 2008; Mattei et al., 2013). Nevertheless, all of them share a common limitation: they are applicable only on a single surfactant class (nonionics, cations etc.). Besides the CMC, similar modeling techniques have been applied to other important surfactant properties like the cloud point of nonionic surfactants or the minimum surface tension at CMC (Hu et al., 2010). Very recently, the first QSPR model for predicting Γ_m was developed (Seddon et al., 2022). The QSPR model was trained on data generated from the Szyszkowski equation using experimentally measured SFT- $\log(c)$ profiles and not on the experimental data directly (Seddon et al., 2022). However, the authors stress that their QSPR model has limitations in the surfactant categories included, e.g., the model is not applicable to fluorinated surfactants (Seddon et al., 2022).

In the recent years, graph neural networks (GNNs) have been intensively researched in the field of molecular property prediction, with numerous GNN models existing in the literature, even regarding the same target property (Yang et al., 2019; Wieder et al., 2020). In more detail, GNNs have been applied to a variety of chemical applications such as ferromagnetic materials (Pasini et al., 2022), the biodegradability of molecules (Rittig et al., 2022) and the activity coefficients (Sanchez Medina et al., 2022; Rittig et al., 2023a; Felton et al., 2022; Rittig et al., 2023b). GNNs are a deep learning technique, where each molecule is represented as a graph, with atoms corresponding to nodes and bonds to edges. In contrast to classical QSPR methods, where molecular descriptors are typically selected manually and therefore require domain knowledge, GNNs can extract, in an automated way, all the necessary structural-related information which are later used in the regression task for property prediction. For surfactants, Qin et al. (2021) used GNNs to predict the CMC of multiple surfactant classes. They showed that GNNs can be efficiently used as an alternative to classical descriptor-based QSPR in surfactants, with very promising results, using a database of 200 molecules, which is relatively small for training a machine learning model.

Herein, we create the largest CMC and Γ_m data sets available and we use them to develop GNN models for their prediction. First, we extend the publicly available CMC data set of Qin et al. (2021) to 429 molecules through an extensive literature search. Then, we construct a second data set of 99 molecules with duplicate values with the aim of investigating possible benefits of transfer learning in CMC prediction. For the Γ_m , no publicly available database was found during our research. Therefore, we construct one with 164 surfactant molecules varying from multiple surfactant class types. Compared to the work of Seddon et al. (2022), we include a wider range of surfactant categories, e.g., fluorinated components, and we consider the impact of counterions on Γ_m (Rosen and Kunjappu, 2012). Note that the collected data sets include only measurements that can be found in various sources of publicly

available literature.

Furthermore, we establish a GNN model for the prediction of surface excess concentration (Γ_m) and a GNN model for the prediction of CMC, both trained on the above mentioned new databases. Additionally, we investigate multi-task learning to overcome data limitations and ensemble learning to enhance the predictive performance. Then, we experimentally measure 3 industrial grade surfactants, previously unseen by the GNN model. Finally, we predict their CMC with our GNN model, which was trained exclusively on literature data with mainly purified surfactants, and demonstrate the model’s ability to generalize to unpurified industrial surfactants.

We construct the rest of this work as following: Firstly, we analyze our databases, data sampling procedure and the industrial surfactants used (Section 2). Thereafter, we give an overview of how GNN models work, the methods we applied and a brief overview of the hyperparameter selection (Section 3). We then present our results, compare them with previous works and discuss limitations and possible solutions (Section 4). Lastly, we summarize our work and suggest possible future improvements (Section 5). The test data used for model evaluation is publicly available in our [GitHub repository](#). The training data set remains property of BASF and could be made available upon request.

2 Data sets

We now analyze the existing databases and describe our methodology for data collection (Section 2.1). Following, we discuss the estimation of CMC and how we handled duplicated values for transfer learning (Section 2.2). Finally, we analyze the collected data sets (Section 2.3) and we present three industrial grade surfactants for model testing (Section 2.4).

2.1 Existing database analysis and data collection

We started our work by building on the publicly available database of 202 substances from [Qin et al. \(2021\)](#) for CMC prediction. For the surface excess concentration Γ_m , we had to exclusively rely on tables in books and publications, such as ([Rosen and Kunjappu, 2012](#); [Dahanayake et al., 1986](#)), because no constructed data set was found in the literature. At first, literature data (CMC and Γ_m) was extracted from multiple sources ([Rosen and Kunjappu, 2012](#); [Gaudin et al., 2016](#); [Mukerjee and Mysels, 1971](#)) for all the molecules at temperatures between 20-28°C. Note that since temperature massively impacts both properties, we only focus on the temperature range defined above. We also traced back to the individual articles referenced in the sources mentioned above ([Rosen and Kunjappu, 2012](#); [Gaudin et al., 2016](#); [Mukerjee and Mysels, 1971](#)) and extracted additional CMC and Γ_m data. This procedure resulted in an extended data set of 429 distinct substances for CMC. In addition, we simultaneously collected 164 different Γ_m values from multiple sources.

2.2 CMC data collection procedure and duplicate values

During data collection, we often found multiple CMC values for the same surfactant, differing from source to source, due to factors such as purity levels, measuring method of choice and mathematical evaluation of experimental data ([Moulik et al., 2021](#); [Perinelli et al., 2020](#)). An example is given in Table 1, where for the same surfactant 4 different values have been reported. The CMC variations are discussed in previous works and remain an issue in surfactant science ([Moulik et al., 2021](#); [Perinelli et al., 2020](#); [Mukerjee and Mysels, 1971](#)).

To handle duplicate values, we decided for a ranking according to the measurement method. Here, we prefer CMC values obtained via tensiometry because one of our targets is to evaluate our model on industrial grade surfactants using CMC values measured through tensiometry. If tensiometry data was not available, we favored data from refractometry measurements since it was found to be reliable by Mukerjee and Mysels ([Mukerjee and Mysels, 1971](#)). If data only from other methods was available, i.e., neither tensiometry nor refractometry, we also included it into our main data set. All remaining values for a surfactant, i.e., duplicates, are not included in the main data set but rather collected in a separate data set, which we utilize for a transfer learning approach (cf. Section 3.5). We note that for most

Tab. 1. CMC values of dodecylpyridinium bromide reported in literature at 25°C.

Method	Value (mM)	Source
Tensiometry	11.5	(Rosen et al., 1982b)
Conductometry	11.3	(Rosen et al., 1982b)
Conductometry	10	(Škerjanc et al., 1999)
Light scattering	11.6	(Ford et al., 1966)

surfactants where duplicate values exist, the values tend to be very similar to each other and in some cases even equal.

2.3 Data sets analysis

The described sampling process in Section 2.2 led us to construct the three data sets shown in Table 2, together with a detailed surfactant class distribution. We observe that in the two main databases, nonionic surfactants is the dominant class followed by anionics. This class distribution matches with consumption data of surfactants in 2000 (Rosen and Kunjappu, 2012; Myers, 2020), where anionic and nonionic surfactants are the most used in industrialized areas. In other words, the research focus is matching the industrial output. Afterwards, a statistical overview of the target properties, i.e. CMC and Γ_m , is presented in Figure 1. We note that Γ_m shows a natural normal distribution without applying the logarithm. Both data sets have similar mean, median, 5th and 95th percentile values although no comparison between them should be made, as CMC values are scaled. The smallest and biggest values in both data sets are similar too. Finally, a correlation plot between log CMC and Γ_m is given in Figure 2, containing surfactants for which both CMC and Γ_m values are collected.

2.4 Industrial Surfactants

With an estimated market size of around \$40 billion in 2020 (Fortune Business Insights, 2021), surfactants are also heavily researched in the industry. As Myers (Myers, 2020) points out, the majority of academic interest in surfactants, focuses generally on highly purified compounds while the industry is either using complex mixtures to obtain the desired performance or unpurified compounds due to economical reasons. For surface properties like CMC, many authors have noticed the effect of impurities on CMC through the years (Mukerjee and Mysels, 1971; Moulik et al., 2021; Patist et al., 2000). In this study, we examine to what extent GNN models trained exclusively on literature data can generalize for unpurified industrial surfactants.

Three industrial-grade pure-component surfactants were used, provided by BASF, as obtained from production site without further purification. The main species in these surfactants are (S1) Texapon 842 UP (Sodium Caprylyl Sulfate), (S2) Texapon EHS (Sodium 2-Ethylhexyl Sulfate) and (S3) Texapon K 12 G (Sodium Dodecyl Sulfate). We exclude those three molecules from the training set. According to manufacturing process, we expect the presence of unreacted raw material, alcohols in this case, and reaction by-products.

Tab. 2. Number of surfactants per class for each database collected in this work. DV = Duplicate Values.

	CMC	Γ_m	DV-CMC
Nonionics	220	86	19
Anionics	130	44	44
Cationics	55	13	27
Zwitterionics	24	21	9
Total substances	429	164	99

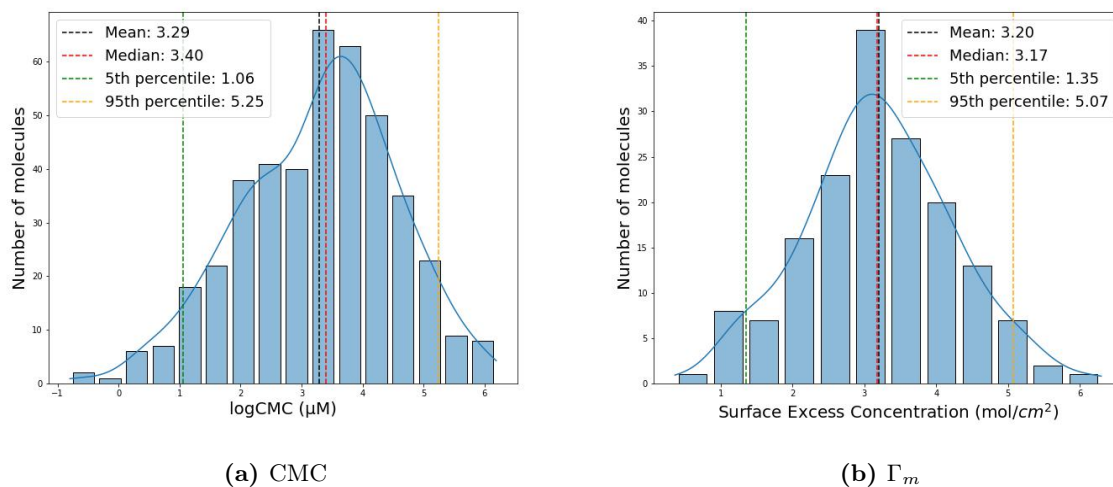


Fig. 1. Statistical overview of CMC and Γ_m databases, assembled from literature in this work. Normal distribution of the data set would ensure an even train-validation-test split without artifact.

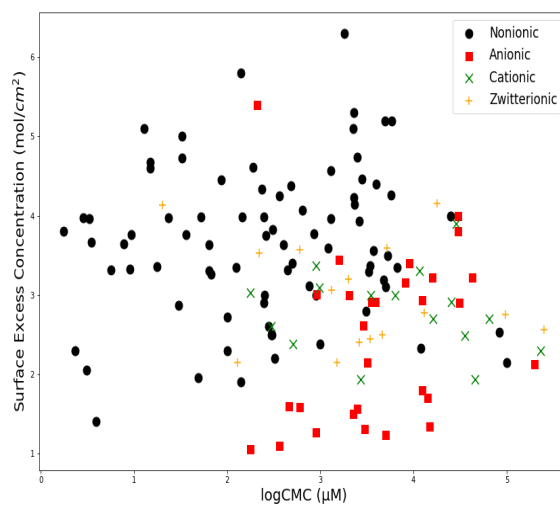


Fig. 2. Correlation plot between \log CMC and Γ_m for all surfactant classes. In the plot, 141 surfactants are presented, for which both CMC and Γ_m data was collected from the literature.

3 Methods

In this section, we first present the fundamentals of a GNN model (Section 3.1), the general training settings of current works (Section 3.2) and the hyperparameter selection (Section 3.3). Afterwards, we refer to the learning techniques applied on this paper (Sections 3.4–3.6). The CMC of the three industrial surfactants was determined by plotting the surface tension as a function of the logarithm of the surfactant concentration. From this plot, two linear regions were determined, which correspond to the linear concentration-dependent and the linear concentration-independent region, respectively. The CMC value is then obtained from the intersection of the straight lines. Finally, for the surface tension measurement a Force Tensiometer – K100 (Krüss, Germany), at 23°C was used.

3.1 Graph Neural Networks

In GNN models, every molecule is treated as an undirected graph, where atoms correspond to nodes and bonds to edges. A feature vector, containing chemical information, is assigned to each atom and each edge. Our node and edge features of choice are shown in Table 3 and Table 4 respectively, motivated from our previous works (Schweidtmann et al., 2020; Rittig et al., 2023a) and past literature (Yang et al., 2019). Please note that hydrogen atoms are not considered as individual nodes but are implicitly represented in the node feature vector. A surfactant example is given in Figure 3. The molecular graph then passes through graph convolutions, where neighbor information, i.e., neighboring node and edge features, is aggregated for each node in the graph accordingly. The network depth L , i.e., the number of graph convolutional layers, defines the neighborhood pool from which structural information will be aggregated. We herein use edge-conditioned graph convolutional layers (Simonovsky and Komodakis, 2017) and a gated recurrent unit (GRU) (Cho et al., 2014), similar to the message passing framework by Gilmer et al. (2017) and our previous works (Schweidtmann et al., 2020; Rittig et al., 2022, 2023a). In contrast to Qin et al. (2021) who used graph convolutional layers only considering node features, we thus explicitly include bond type information in learning the molecular structure which potentially facilitates distinguishing molecules with similar heavy atoms but different bonds, e.g., alkanes versus alkenes. After the last graph convolutional layer, the final updated atom feature vectors are pooled into a final molecular fingerprint vector \mathbf{h}_{FP} (Gilmer et al., 2017) through a permutation invariant function, i.e., summation of all node vectors. The \mathbf{h}_{FP} contains all the necessary structure-related information of a specific molecule required for molecular property prediction, thereby replacing the selected descriptors in classical QSPR techniques mentioned in Section 1.

Our model is implemented in the Pytorch Geometric (PyG) framework (Fey and Lenssen, 2019). For the attributed molecular graph generation, we use the SMILES string (Weininger, 1988) of each molecule and RDKit (*version 2022.3.5*), an open-source toolkit for cheminformatics.

3.2 General training settings

We use the high-quality data set CMC to define the hyperparameters of our GNN models. For the target property CMC, the log CMC is calculated and then standardized to a zero mean and a standard deviation of one. The train and test sets are separated randomly in a 85% - 15% ratio respectively. For the hyperparameter selection an internal validation set is used, which is a subset of the training set with 20 substances each. The loss function is the mean squared error (MSE) and the optimizer is Adam (Kingma and Ba, 2014). In general, we use the same general training settings as in our previous works (Schweidtmann et al., 2020; Rittig et al., 2023a) and the interested reader can refer to them for more information. For every modeling approach, which will be introduced in Sections 3.4–3.6, as well as in industrial surfactants application, 40 models were trained on 40 individual training subsets and the results are averaged and reported in Section 4.

3.3 Hyperparameter selection

With the hyperparameter selection procedure, the aim is to find the suitable hyperparameters of our GNN model. For a robust hyperparameter selection, we test each model in 40 different internal validation sets.

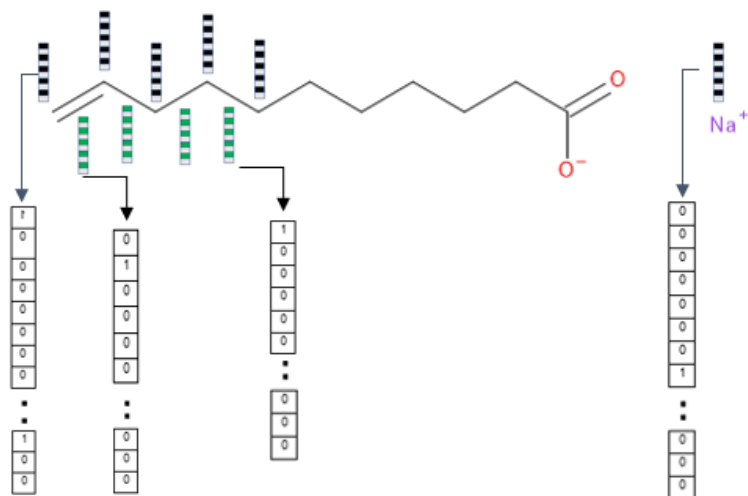


Fig. 3. A surfactant molecule represented as underdirected graph. In every node (atom) a feature vector (black-white color) of size 30 and in every edge (bond) a feature vector (green-white) of size 12 is assigned. The feature vectors encode chemical information about each individual atom and edge respectively. As can be seen in the atom features vector, different atoms have different entries, which distinguishes them from the other atoms. Similarly, bonds are distinguished through their feature vector too.

Tab. 3. Atom features used in the molecular graph representation. All features are implemented as one-hot-encoding.

Feature	Description	Dimension
atom type	atom type (C, N, O, S, F, Cl, Br, Na, I, B, K, H, Li)	13
is aromatic	if the atom is part of an aromatic system	1
hybridization	sp, sp ² , sp ³ , sp ³ d, or sp ³ d ²	5
# bonds	number of bonds the atom is involved in	6
# Hs	number of bonded hydrogen atoms	5
Total		30

Tab. 4. Edge features used in the molecular graph representation. All features are implemented as one-hot-encoding.

Feature	Description	Dimension
bond type	single, double, triple, or aromatic	4
is in a ring	whether the bond is part of a ring	1
conjugated	whether the bond is conjugated	1
stereo	none, any, E/Z, or cis/trans	6
Total		12

We perform a grid search for the following hyperparameters of the GNN model, varying them within the respective ranges: Graph convolutional type $\in \{NNConv, GINEConv\}$, number of graph convolutional layers $\in \{1, 2, 3\}$, usage of GRU $\in \{True, False\}$, the batch size $\in \{4, 8, 16\}$, the initial learning rate $\in \{0.005, 0.01, 0.05\}$, dimensions of molecular fingerprint and of MLP $\in \{64, 128, 256\}$. In other words, the hidden layers of the graph convolution part and the hidden layers of the MLP are always the same size. The optimum combination is a GNN architecture with an initial learning rate of 0.005, a hidden state size of 64, a batch size of 16, total graph convolutional layers of 1, the NNConv graph convolutional type and the usage of GRU for the message passing scheme. Our edge feature network, similar to our previous work (Schweidtmann et al., 2020), consists three layers with the following number of neurons: #1: 12, #2: 64, and #3: 4096. The architecture exhibits 306,561 learnable parameters in total.

3.4 Single- and Multi-task Learning

A surfactant molecule usually has multiple target properties, as we discussed above in Section 1. The classical learning approach, *single-task learning*, is to train individual models for every property of interest. In single-task learning, model parameters are directly optimized based exclusively on a single target property only, and not transferred to another property prediction task. In that sense, all available QSPR methods for surfactants (discussed in Section 1) are single-task learning. On the other hand, in *multi-task learning* multiple target properties are simultaneously predicted (Caruana, 1997; Zhang and Yang, 2017). The simultaneous prediction has been shown to improve the modeling accuracy of GNNs in molecular property prediction (Schweidtmann et al., 2020; Capela et al., 2019; Pasini et al., 2022). Normally during multi-task learning, the graph convolutional layers are shared and individual MLPs are constructed for each target property. The benefits of this approach, are mainly models’ ability to generalize, learn faster, reduce overfitting (Ruder, 2017; Crawshaw, 2020) and data efficiency (Crawshaw, 2020).

In the present work, we investigate the prediction of CMC and of Γ_m with both single- and multi-task learning. Specifically, we develop a single-task learning model for each property individually and multi-task learning models for simultaneous prediction of the properties. Since both of the properties come from the same measurement procedure and therefore are correlated, we expect an improved model accuracy during multi-task learning.

3.5 Transfer Learning

Another technique for improving machine learning models is transfer learning (Hendrycks et al., 2019; Zhuang et al., 2020). During transfer learning, a model is usually pre-trained on a data set, for example a synthetic one, and then the model parameters are used to initialize the training on a new unseen data set. This technique is very useful when only small data sets are available. In the field of GNNs, researchers investigated the benefits and limitations of transfer learning (Grambow et al., 2019; Han et al., 2021; Kooverjee et al., 2022).

As we described in Section 2.2, we collect duplicate values to apply transfer learning to single-task CMC prediction, with the scope of utilizing bigger portions of experimental data from the literature. We use the data set DV-CMC (Table 2) to pre-train the model, i.e., learn the graph convolutions and MLP parameters, and afterwards we initiate our single-task CMC model with them. All the initialized parameters are optimized based on the CMC data set (Table 2).

3.6 Ensemble Learning

Training and using single models can lead to under- or/and over-predictions. A well-known technique to mitigate this phenomenon in machine learning is ensemble learning (Breiman, 1996; Dietterich, 2000). In ensemble learning, multiple models are trained on different subsets of training data set and their final predictions are averaged, resulting in more robust and generalized predictions (Breiman, 1996; Dietterich, 2000; Ganaie et al., 2022).

We use ensemble learning both for our single- and multi-task models mentioned in Section 3.4, by training 40 different models in 40 different subsets of our training data set, in each case. Afterwards, we

Tab. 5. Summary of model accuracy for different predictive tasks over 40 different runs. In each case the standard deviation is also given, except ensemble learning. In the above table we use the following abbreviations: STL = single-task learning, MTL= multi-task learning, TL = transfer learning, EL = ensemble learning, MAE = mean absolute error, RMSE = root mean squared error.

	CMC		Γ_m	
	RMSE	MAE	RMSE	MAE
STL (val)	0.27 \pm 0.027	0.2 \pm 0.026	1.02 \pm 0.169	0.85 \pm 0.15
STL (test)	0.33 \pm 0.033	0.25 \pm 0.026	0.8 \pm 0.143	0.57 \pm 0.146
STL & TL (val)	0.27 \pm 0.034	0.2 \pm 0.033		
STL & TL (test)	0.33 \pm 0.042	0.26 \pm 0.034		
MTL (val)	0.26 \pm 0.075	0.2 \pm 0.053	0.3 \pm 0.121	0.26 \pm 0.116
MTL (test)	0.36 \pm 0.041	0.27 \pm 0.031	0.59 \pm 0.051	0.43 \pm 0.044
STL & EL (test)	0.28	0.21	0.76	0.53
MTL & EL (test)	0.31	0.23	0.56	0.4

use the 40 different models to perform predictions in our test set, which are averaged to obtain the final scores.

4 Results & Discussion

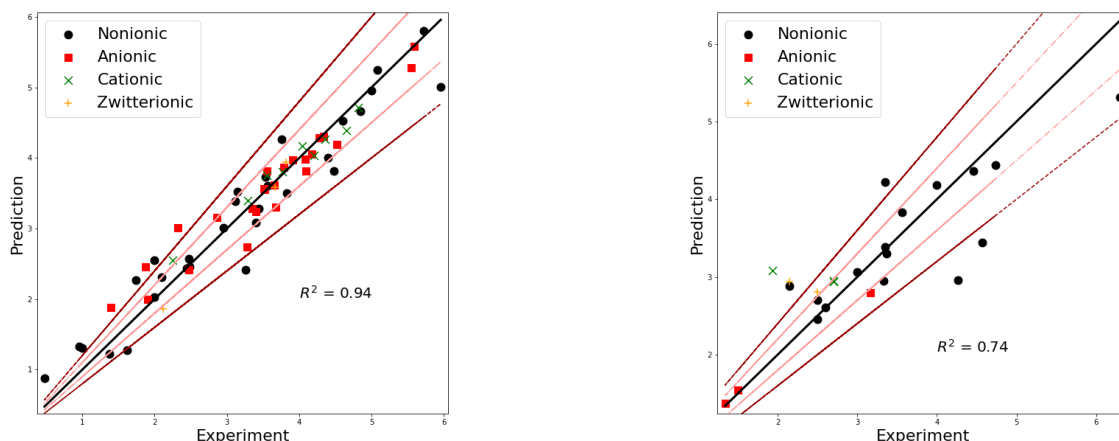
In this section, we firstly summarize the predictive performance of our models (Section 4.1). Afterwards we compare our findings with previous similar work (Section 4.2) and finally we conclude with investigation of model applicability on the selected industrial surfactants (Section 4.3). An overview of the performance of the developed models is reported in Table 5. For every task we report the root mean squared error (RMSE), the mean absolute error (MAE) and the variances on the validation and test sets.

4.1 Predictive performance

The single-task GNN model for CMC exhibits an average RMSE of 0.27 on validation set and 0.33 on test set, while the variance is bigger in the test set than in the validation set. For Γ_m the average RMSE in test set is lower than the one in the validation set, with the former equal to 0.85 and the later equal to 1.02. Using the logarithm of Γ_m did not improve the performance. Our model exhibits great performance in predicting the log CMC, but fails to exhibit similar performance in Γ_m prediction. The reason for the model’s under-performance may be the small size of the data set used (140 molecules) for the training and the ambiguous measuring procedures.

In multi-task learning, the GNN model for CMC prediction exhibits an average RMSE of 0.26 on validation set and 0.36 on test set. For Γ_m prediction, the average RMSE in test set is again lower than the one in the validation set, with the former equal to 0.59 and the later equal to 0.43. In the CMC task, the model perform identical with the one in single-task learning, both for validation and test sets, while in the Γ_m task the multi-task model exhibits significantly better performance on the validation set, with the RMSE reducing by 60%, and improved performance on the test set, with the RMSE reducing by 20%. Therefore, we conclude that the data limitations of the Γ_m database as single target property can be overcome by applying multi-task learning. On the other hand, the CMC model did not benefit from the additional data and showed identical results with a slightly higher variance but an overall similar accuracy compared to the single-task learning.

The transfer learning approach, i.e., pre-training the model using the 99 collected duplicate values described in Section 2.2, is applied only on the single-task CMC model. The RMSE on the validation set remains the same as in single-task learning, equal to 0.27 and on the test set equal to 0.33. Interestingly, the standard deviation increases in both sets. The increase may be due to the broader range of target values for the same property, which leads the model to deviate more from the true value. We observed that transfer learning slightly reduced the final model training time, i.e., the model reached its optimum



(a) CMC test set: Predicted versus experimental value of $\log(\text{CMC})$ in μM .

(b) Γ_m test set Predicted versus experimental value of Γ_m in mol/cm^2 .

Fig. 4. Multi-task GNN ensemble models for (a) CMC and (b) Γ_m for all surfactant classes. The light red dashed lines represent the 10% error and the dark red dashed lines the 20% error.

sooner. Besides the slight reduction of final model training time, using duplicate values for transfer learning led to similar performance.

Ensemble learning, i.e., averaging the predictions of the 40 trained models, slightly reduces the RMSE on test set for single-task learning to 0.28 and for multi-task learning to 0.31 in the CMC case. A similar RMSE reduction is observed on test set for Γ_m accordingly, to 0.76 for single-task learning and to 0.56 for multi-task learning. We use the ensembled results in multi-task CMC and Γ_m learning to draw the parity plots (measured vs predicted values) for CMC and Γ_m show a high determination coefficient for the former, $R^2_{\text{CMC}} = 0.94$, and moderate one for the latter $R^2_{\Gamma_m} = 0.74$. We demonstrate that the GNN approach in the present work, can predict CMC and Γ_m across all surfactant classes.

In addition, we present the three components with the highest absolute CMC error in Figure 5. For molecule one, the combination of high CMC value and lack of similar molecules, i.e. small alkyl chain with high number of ethylene oxides in the training set, may be the reasons why the model fails to perform well. For molecules two and three, we suspect the measurement may have an impact on the result since identical molecules can be found in the training set.

Similarly, the four components with the highest absolute Γ_m error are illustrated in Figure 6. Molecule four is similar as in the CMC case, which supports the measurement impacted hypothesis from before. On the other side molecules one and three have complex structure, where at a similar chemistry is lacking in the training set. Therefore, we can assume that the model fails to capture the property-structure relationship in this case. The same reasoning can be applied to molecule two, where we also lack similar molecules in the training set.

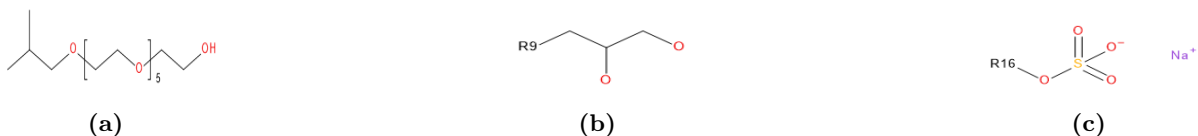


Fig. 5. Outliers in multi-task learning for CMC prediction. Two of them, (a) and (b) belong to nonionic class and the third, (c) to anionic class.

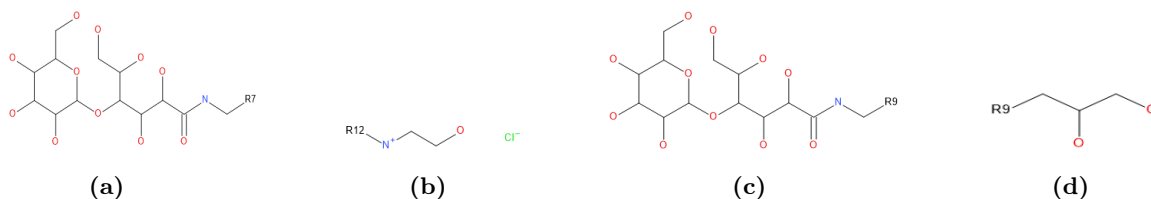


Fig. 6. Outliers in multi-task learning for Γ_m prediction. Three of them, (a), (c) and (d) belong to nonionic class and the second, (b) to cationic class.

4.2 Comparison with previous works

We next compare our results to the work of [Qin et al. \(2021\)](#) and their GNN model for CMC prediction, which used a subset of our CMC training data but is also applicable for a wide choice of surfactant classes. [Qin et al. \(2021\)](#) report a test RMSE of 0.30 which is similar to ours of 0.28. Note that our test set is almost three times the size of the one used by [Qin et al. \(2021\)](#), so that we cover a higher variance of molecules. Besides the slight RMSE improvement in test set, our model reduces also the average RMSE on the validation set from 0.39 to 0.27. As can be seen in [Figure 7](#), no major outliers were observed in the 40 models. Finally, most of the models exhibited a test RMSE in the range of 0.26-0.29 while [Qin et al. \(2021\)](#) reported a broader test RMSE range of 0.28-0.45.

Overall, the comparison shows that the general performance of our model on the CMC is similarly high with previous ones, although a direct quantitative comparison is not possible due to the different data sets used. As there is no model for predicting surface excess concentration directly from experimental data (cf. [Section 1](#)), we are unable to compare our results for Γ_m with other works.

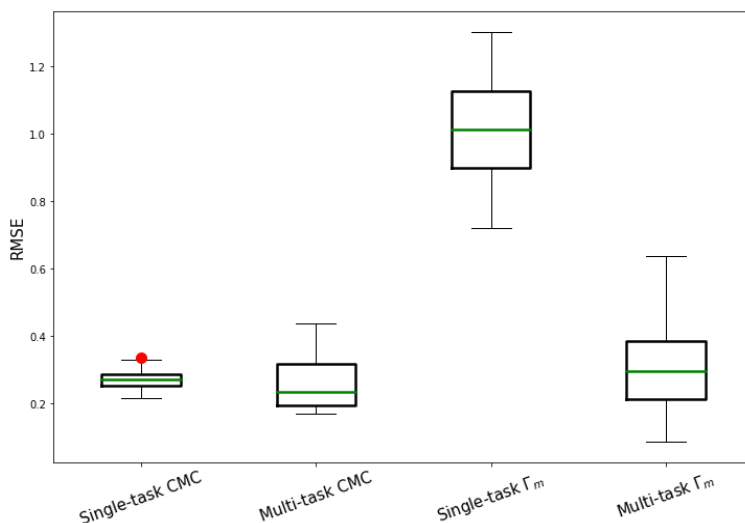


Fig. 7. Distribution plot of RMSE on internal validation set for all the learning tasks. The boxplots are the results of 40 runs in different internal validation sets. The red points represent the outliers.

4.3 Industrial Surfactants

We then apply our developed GNN model to predict on the three pure component industrial surfactants described in [Section 2.4](#). According to the above discussed results, the best learning approach for CMC is the combination of single-task with ensemble learning. We use the 40 trained models from [Section 4.1](#) to perform ensemble predictions on the three surfactants. The predicted log CMC values, as well the experimental measured ones, are given in [Table 6](#) for comparison. For all of the three, the predicted values

Tab. 6. Comparison of predicted values from our single-task GNN with ensemble versus experimentally calculated values for three selected industrial grade surfactants. For the predicted values, the standard deviation over 40 individual runs is also given. The above values, are the logarithmic ones.

	Predicted CMC (μM)	Measured CMC (μM)
S1	4.87 ± 0.11	4.88
S2	4.95 ± 0.17	4.98
S3	3.91 ± 0.08	3.86

are very close to the measured ones. Overall, the data indicates that the developed GNN model trained on literature data can accurately predict the CMCs for all three single-molecule industrial unpurified surfactants.

We note that similar molecules are used in the training set and none of the three exhibits high structural complexity. On the other hand, the impurities effects on CMC are not learnt from the model and their implementation could potentially be future area of research. Future work could also focus on testing the applicability of GNN model in research of bio-surfactants, with many of them naturally exhibit high structural complexity.

5 Conclusions and future work

We apply GNNs to pure component surfactants to predict CMC and Γ_m . Based on extensive literature scanning, we generate a database for CMC with double the size of existing. We also construct a data set for Γ_m . As GNNs have been successfully used for CMC prediction (Qin et al., 2021), we extend the GNN architecture to simultaneously predict the surface excess concentration Γ_m in a multi-task learning, thereby utilizing correlations between these two properties. Furthermore, we collect additional CMC values from the literature and investigate if transfer learning can increase the model accuracy.

All GNN models exhibit high-accuracy CMC predictions, on a comparable level to a recently developed GNN model by Qin et al. (2021) but for an extended spectrum of surfactants. For Γ_m on the other hand, the single-task GNNs fail to capture the property-structure relationship; here, we find that multi-task GNNs effectively utilizes the CMC data to substantially enhance prediction accuracy for Γ_m . In all cases, ensemble learning increases the prediction accuracy. For transfer learning, however, we observe no improvements in the model accuracy. Finally, we test the best GNN model for CMC on three unpurified industrial surfactants and find highly accurate predictions matching our laboratory measurements, thereby indicating strong potential for further industrial applications.

Furthermore, our GNN models are subject to certain limitations. As is typically the case for ML models, the applicability of our GNN models is limited to surfactants with similar structure as the ones contained in the training data set. Stereochemistry is also not taken into account in this work, for example in the case of n-dodecyl-D-maltoside we only use the CMC of the α isomer (Pagliano et al., 2012). Another limitation, shortly mentioned above, is not including information regarding the purity of each compound. We only considered highly purified compounds reported in literature and future research should focus in incorporating surface active impurities to the GNN model.

Future work could extend the relative small database for surface excess concentration Γ_m , thus yielding higher performance predictive models. For Γ_m noise is often encountered in reported values due to it is implicit calculation through various approaches of the Gibbs adsorption equation (Rosen and Kunjappu, 2012). This noise prohibits the GNN model to better capture the structure-property relationship. Finally, prediction of further surfactant properties based on the structure would be highly interesting for surfactant formulators.

Acknowledgments

The BASF authors (C. Brozos, S. Bhattacharya, E. Akanny and C. Kohlmann) were funded by the BASF Personal Care and Nutrition GmbH. J. G. Rittig and A. Mitsos acknowledge funding from the Deutsche Forschungsgemeinschaft (DFG, German Research Foundation) – 466417970 – within the Priority Programme “SPP 2331: Machine Learning in Chemical Engineering”. Additionally, J. G. Rittig acknowledges the support of the Helmholtz School for Data Science in Life, Earth and Energy (HDS-LEE).

Data availability

All python scripts and the test data used in this work are available as open-source at <https://github.com/brozosc/Graph-Neural-Networks-for-Surfactant-Multi-Property-Prediction>.

Author contribution

Christoforos Brozos: Conceptualization, Methodology, Software, Data curation, Validation, Formal analysis, Writing - Original Draft, Writing - Review & Editing, Visualization

Jan G. Rittig: Conceptualization, Methodology, Software, Formal analysis, Writing - Review & Editing

Sandip Bhattacharya: Conceptualization, Methodology, Formal analysis, Supervision, Writing - Review & Editing

Elie Akanny: Conceptualization, Methodology, Experimental methodology & measurements, Writing - Review & Editing

Christina Kohlmann: Writing - Review & Editing, Supervision, Funding acquisition

Alexander Mitsos: Writing - Review & Editing, Supervision, Funding acquisition

Bibliography

- Adu, S. A., Naughton, P. J., Marchant, R., and Banat, I. M. (2020). Microbial biosurfactants in cosmetic and personal skincare pharmaceutical formulations. *Pharmaceutics*, 12.
- Al-Sabagh, A., Nasser, N., Migahed, M., and Kandil, N. (2011). Effect of chemical structure on the cloud point of some new non-ionic surfactants based on bisphenol in relation to their surface active properties. *Egyptian Journal of Petroleum*, 20(2):59–66.
- Breiman, L. (1996). Bagging predictors. *Machine Learning*, 24(2):123–140.
- Capela, F., Nouchi, V., Deursen, R. V., Tetko, I. V., and Godin, G. (2019). Multitask learning on graph neural networks applied to molecular property predictions. arXiv preprint arXiv:1910.13124.
- Caruana, R. (1997). Multitask learning. *Machine Learning*, 28(1):41–75.
- Cho, K., van Merriënboer, B., Gulcehre, C., Bahdanau, D., Bougares, F., Schwenk, H., and Bengio, Y. (2014). Learning phrase representations using rnn encoder-decoder for statistical machine translation. arXiv preprint arXiv:1406.1078.
- Crawshaw, M. (2020). Multi-task learning with deep neural networks: A survey. arXiv preprint arXiv:2009.09796.
- Dahanayake, M., Cohen, A. W., and Rosen, M. J. (1986). Relationship of structure to properties of surfactants. 13. surface and thermodynamic properties of some oxyethylenated sulfates and sulfonates. *J. Phys. Chem.*, 90(11):2413–2418.
- Dietterich, T. G. (2000). Ensemble methods in machine learning. In *Proceedings of the First International Workshop on Multiple Classifier Systems, MCS '00*, page 1–15, Berlin, Heidelberg. Springer-Verlag.
- Felton, K. C., Ben-Safar, H., and Alexei, A. A. (2022). Deepgamma: A deep learning model for activity coefficient prediction. *1st Annual AAAI Workshop on AI to Accelerate Science and Engineering (AI2ASE)*.
- Fey, M. and Lenssen, J. E. (2019). Fast graph representation learning with pytorch geometric. arXiv preprint arXiv:1903.02428v3.
- Ford, W., Ottewill, R., and Parreira, H. (1966). Light-scattering studies on dodecylpyridinium halides. *Journal of Colloid and Interface Science*, 21(5):522–533.
- Fortune Business Insights (2021). Surfactants Market Size, Share & COVID-19 Impact Analysis, By Type (Anionic, Nonionic, Cationic, and Amphoteric), By Application (Home Care, Personal Care, Textile, Food & Beverages, Industrial & Institutional Cleaning, Plastics, and Others), and Regional Forecast, 2021-2028. <https://www.fortunebusinessinsights.com/surfactants-market-102385> (accessed 30-12-2023).
- Gallou, F., Isley, N., Ganic, A., Onken, U., and Parmentier, M. (2015). Surfactant technology applied toward an active pharmaceutical ingredient: more than a simple green chemistry advance. *Green Chem.*, 18.
- Ganaie, M., Hu, M., Malik, A., Tanveer, M., and Suganthan, P. (2022). Ensemble deep learning: A review. *Engineering Applications of Artificial Intelligence*, 115:105151.
- Gaudin, T., Rotureau, P., Pezron, I., and Fayet, G. (2016). New qspr models to predict the critical micelle concentration of sugar-based surfactants. *Ind. Eng. Chem. Res.*, 55(45):11716–11726.
- Ghezzi, M., Pescina, S., Padula, C., Santi, P., Del Favero, E., Cantù, L., and Nicoli, S. (2021). Polymeric micelles in drug delivery: An insight of the techniques for their characterization and assessment in biorelevant conditions. *Journal of Controlled Release*, 332:312–336.

- Gilmer, J., Schoenholz, S. S., Riley, P. F., Vinyals, O., and Dahl, G. E. (2017). Neural message passing for quantum chemistry. *34th International Conference on Machine Learning, ICML 2017*, 3:2053–2070.
- Grambow, C., Li, Y.-P., and Green, W. H. (2019). Accurate thermochemistry with small data sets: A bond additivity correction and transfer learning approach. *J. Phys. Chem. A*, 123(27):5826–5835.
- Han, X., Huang, Z., An, B., and Bai, J. (2021). Adaptive transfer learning on graph neural networks. In *Proceedings of the 27th ACM SIGKDD Conference on Knowledge Discovery & Data Mining, KDD '21*, page 565–574, New York, NY, USA. Association for Computing Machinery.
- Hendrycks, D., Lee, K., and Mazeika, M. (2019). Using pre-training can improve model robustness and uncertainty. In Chaudhuri, K. and Salakhutdinov, R., editors, *Proceedings of the 36th International Conference on Machine Learning*, volume 97 of *Proceedings of Machine Learning Research*, pages 2712–2721. PMLR.
- Hu, J., Zhang, X., and Wang, Z. (2010). A review on progress in qspr studies for surfactants. *International journal of molecular sciences*, 11:1020–47.
- Jobe, D. J. and Reinsborough, V. C. (1984). Micellar properties of sodium alkyl sulfoacetates and sodium dialkyl sulfosuccinates in water. *Canadian Journal of Chemistry*, 62:280–284.
- Katritzky, A. R., Pacureanu, L. M., Slavov, S. H., Dobchev, D. A., and Karelson, M. (2008). Qspr study of critical micelle concentrations of nonionic surfactants. *Ind. Eng. Chem. Res.*, 47(23):9687–9695.
- Škerjanc, J., Kogej, K., and Cerar, J. (1999). Equilibrium and transport properties of alkylpyridinium bromides. *Langmuir*, 15(15):5023–5028.
- Kingma, D. P. and Ba, J. (2014). Adam: A method for stochastic optimization. arXiv preprint arXiv:1412.6980.
- Knop, K., Hoogenboom, R., Fischer, D., and Schubert, U. (2010). Poly(ethylene glycol) in drug delivery: Pros and cons as well as potential alternatives. *Angewandte Chemie International Edition*, 49(36):6288–6308.
- Kooverjee, N., James, S., and van Zyl, T. (2022). Investigating transfer learning in graph neural networks. *Electronics*, 11(8).
- Kumar, A. and Mandal, A. (2019). Critical investigation of zwitterionic surfactant for enhanced oil recovery from both sandstone and carbonate reservoirs: Adsorption, wettability alteration and imbibition studies. *Chemical Engineering Science*, 209:115222.
- Majeed, T., Sølling, T. I., and Kamal, M. S. (2020). Foamstability: The interplay between salt-, surfactant- and critical micelle concentration. *Journal of Petroleum Science and Engineering*, 187:106871.
- Mattei, M., Kontogeorgis, G. M., and Gani, R. (2013). Modeling of the critical micelle concentration (cmc) of nonionic surfactants with an extended group-contribution method. *Ind. Eng. Chem. Res.*, 52(34):12236–12246.
- Moulik, S. P., Rakshit, A. K., and Naskar, B. (2021). Evaluation of non-ambiguous critical micelle concentration of surfactants in relation to solution behaviors of pure and mixed surfactant systems: A physicochemical documentary and analysis. *Journal of Surfactants and Detergents*, 24(4):535–549.
- Mukerjee, P. and Mysels, K. J. (1971). Critical micelle concentrations of aqueous surfactant systems. Technical report, National Standard reference data system.
- Myers, D. (August 2020). *Surfactant Science and Technology, 4th Edition*. John Wiley & Sons, Ltd.
- Nitschke, M. and Costa, S. (2007). Biosurfactants in food industry. *Trends in Food Science & Technology*, 18(5):252–259.

- Ortona, O., Vitagliano, V., Paduano, L., and Costantino, L. (1998). Microcalorimetric study of some short-chain nonionic surfactants. *Journal of Colloid and Interface Science*, 203(2):477–484.
- Pagliano, C., Barera, S., Chimirri, F., Saracco, G., and Barber, J. (2012). Comparison of the α and β isomeric forms of the detergent n-dodecyl-d-maltoside for solubilizing photosynthetic complexes from pea thylakoid membranes. *Biochimica et Biophysica Acta (BBA) - Bioenergetics*, 1817(8):1506–1515. Photosynthesis Research for Sustainability: From Natural to Artificial.
- Pasini, M. L., Zhang, P., Reeve, S. T., and Choi, J. Y. (2022). Multi-task graph neural networks for simultaneous prediction of global and atomic properties in ferromagnetic systems*. *Machine Learning: Science and Technology*, 3(2):025007.
- Patist, A., Bhagwat, S. S., Penfield, K. W., Aikens, P., and Shah, D. O. (2000). On the measurement of critical micelle concentrations of pure and technical-grade nonionic surfactants. *Journal of Surfactants and Detergents*, 3(1):53–58.
- Patist, A., Oh, S., Leung, R., and Shah, D. (2001). Kinetics of micellization: Its significance to technological processes. *Colloids and Surfaces A: Physicochemical and Engineering Aspects*, 176:3–16.
- Perinelli, D. R., Cespi, M., Casettari, L., Vllasaliu, D., Cangiotti, M., Ottaviani, M. F., Giorgioni, G., Bonacucina, G., and Palmieri, G. F. (2016). Correlation among chemical structure, surface properties and cytotoxicity of n-acyl alanine and serine surfactants. *European Journal of Pharmaceutics and Biopharmaceutics*, 109:93–102.
- Perinelli, D. R., Cespi, M., Lorusso, N., Palmieri, G. F., Bonacucina, G., and Blasi, P. (2020). Surfactant self-assembling and critical micelle concentration: One approach fits all? *Langmuir : the ACS journal of surfaces and colloids*, 36:5745–5753.
- Perumal, S., Atchudan, R., and Lee, W. (2022). A review of polymeric micelles and their applications. *Polymers*, 14.
- Qin, S., Jin, T., Van Lehn, R. C., and Zavala, V. M. (2021). Predicting critical micelle concentrations for surfactants using graph convolutional neural networks. *The Journal of Physical Chemistry. B*, 125:10610–10620.
- Rittig, J. G., Ben Hicham, K., Schweidtmann, A. M., Dahmen, M., and Mitsos, A. (2023a). Graph neural networks for temperature-dependent activity coefficient prediction of solutes in ionic liquids. *Computers and Chemical Engineering*, 171:108153.
- Rittig, J. G., Felton, K. C., Lapkin, A. A., and Mitsos, A. (2023b). Gibbs-Duhem-informed neural networks for binary activity coefficient prediction. *Digital Discovery*, 2:1752–1767.
- Rittig, J. G., Gao, Q., Dahmen, M., Mitsos, A., and Schweidtmann, A. M. (2022). Graph neural networks for the prediction of molecular structure-property relationships. arXiv preprint arXiv:2208.04852.
- Rosen, M. and Kunjappu, J. (2012). *Surfactants and Interfacial Phenomena: Rosen/Surfactants 4E*. John Wiley & Sons, Ltd.
- Rosen, M. J., Cohen, A. W., Dahanayake, M., and Hua, X. Y. (1982a). Relationship of structure to properties in surfactants. 10. surface and thermodynamic properties of 2-dodecyloxypoly(ethenoxyethanol)s, c12h25(oc2h4)xoh, in aqueous solution. *J. Phys. Chem.*, 86(4):541–545.
- Rosen, M. J., Dahanayake, M., and Cohen, A. W. (1982b). Relationship of structure to properties in surfactants. 11. surface and thermodynamic properties of n-dodecyl-pyridinium bromide and chloride. *Colloids and Surfaces*, 5(2):159–172.
- Ruder, S. (2017). An overview of multi-task learning in deep neural networks. arXiv preprint arXiv:1706.05098.

- Sanchez Medina, E. I., Linke, S., Stoll, M., and Sundmacher, K. (2022). Graph neural networks for the prediction of infinite dilution activity coefficients. *Digital Discovery*, 1:216–225.
- Schramm, L., Stasiuk, E., and Marangoni, G. (2003). Surfactants and their applications. *Annu. Rep. Prog. Chem., Sect. C: Phys. Chem.*, 99:3–48.
- Schweidtmann, A. M., Rittig, J. G., König, A., Grohe, M., Mitsos, A., and Dahmen, M. (2020). Graph neural networks for prediction of fuel ignition quality. *Energy & Fuels*, 34(9):11395–11407.
- Seddon, D., Müller, E. A., and Cabral, J. T. (2022). Machine learning hybrid approach for the prediction of surface tension profiles of hydrocarbon surfactants in aqueous solution. *Journal of Colloid and Interface Science*, 625:328–339.
- Shaban, S. M., Kang, J., and Kim, D.-H. (2020). Surfactants: Recent advances and their applications. *Composites Communications*, 22:100537.
- Simonovsky, M. and Komodakis, N. (2017). Dynamic edge-conditioned filters in convolutional neural networks on graphs. In *2017 IEEE Conference on Computer Vision and Pattern Recognition (CVPR)*, pages 29–38.
- Su, H., Wang, F., Ran, W., Zhang, W., Dai, W., Wang, H., Anderson, C. F., Wang, Z., Zheng, C., Zhang, P., Li, Y., and Cui, H. (2020). The role of critical micellization concentration in efficacy and toxicity of supramolecular polymers. *Proceedings of the National Academy of Sciences of the United States of America*, 117:4518–4526.
- Szűts, A. and Szabó-Révész, P. (2012). Sucrose esters as natural surfactants in drug delivery systems—a mini-review. *International Journal of Pharmaceutics*, 433(1):1–9.
- Tadros, T. (2005). *Surfactants in Personal Care and Cosmetics*, chapter 12, pages 399–432. John Wiley & Sons, Ltd.
- Thiruvengadam, S., Murphy, M., Tan, J. S., and Miller, K. (2020). A generalized theoretical model for the relationship between critical micelle concentrations, pressure, and temperature for surfactants. *Journal of Surfactants and Detergents*, 23(2):273–303.
- Thompson, C. J., Ainger, N., Starck, P., Mykhaylyk, O. O., and Ryan, A. J. (2023). Shampoo science: A review of the physiochemical processes behind the function of a shampoo. *Macromolecular Chemistry and Physics*, 224(3):2200420.
- Vieira, I. M. M., Santos, B. L. P., Ruzene, D. S., and Silva, D. P. (2021). An overview of current research and developments in biosurfactants. *Journal of Industrial and Engineering Chemistry*, 100:1–18.
- Wang, Z., Chen, Y., Zhang, F., and Lin, S. (2019). Significance of surface excess concentration in the kinetics of surfactant-induced pore wetting in membrane distillation. *Desalination*, 450:46–53.
- Weininger, D. (1988). Smiles, a chemical language and information system. 1. introduction to methodology and encoding rules. *J. Chem. Inf. Comput. Sci.*, 28(1):31–36.
- Wieder, O., Kohlbacher, S., Kuenemann, M., Garon, A., Ducrot, P., Seidel, T., and Langer, T. (2020). A compact review of molecular property prediction with graph neural networks. *Drug Discovery Today: Technologies*, 37:1–12.
- Yang, K., Swanson, K., Jin, W., Coley, C., Eiden, P., Gao, H., Guzman-Perez, A., Hopper, T., Kelley, B., Mathea, M., Palmer, A., Settels, V., Jaakkola, T., Jensen, K., and Barzilay, R. (2019). Analyzing learned molecular representations for property prediction. *Journal of Chemical Information and Modeling*, 59(8):3370–3388. PMID: 31361484.
- Yang, Z. and Brouillette, C. G. (2016). Chapter thirteen - a guide to differential scanning calorimetry of membrane and soluble proteins in detergents. In Feig, A. L., editor, *Calorimetry*, volume 567 of *Methods in Enzymology*, pages 319–358. Academic Press.

- Zhang, F., Li, S., Zhang, Q., Liu, J., Zeng, S., Liu, M., and Sun, D. (2019). Adsorption of different types of surfactants on graphene oxide. *Journal of Molecular Liquids*, 276:338–346.
- Zhang, Y. and Yang, Q. (2017). A survey on multi-task learning. *IEEE Transactions on Knowledge and Data Engineering*, 34:5586–5609.
- Zhuang, F., Qi, Z., Duan, K., Xi, D., Zhu, Y., Zhu, H., Xiong, H., and He, Q. (2020). A comprehensive survey on transfer learning. *Proceedings of the IEEE*, PP:1–34.